Crack Propagation on ESE(T) Specimens Strengthened with CFRP Sheets

Hansen, Christian Skodborg; Jensen, Peter Holmstrøm; Dyrelund, Jens; Täljsten, Björn

Published in:
Advanced Composites in Conctruction 2009

Publication date:
2009

Document Version
Publisher's PDF, also known as Version of record

Crack Propagation in ESE(T) Specimens Strengthened with CFRP Sheets

Christian S. Hansen, Peter H. Jensen,
Jens Dyrelund and Björn Täljsten
Technical University of Denmark
Department of Civil Engineering
Brovej, Bygning 118, 2800 Kgs. Lyngby, Denmark

ABSTRACT

In this paper fatigue tests on side notched steel test specimens strengthened with adhesive bonded fibre reinforced polymer (FRP) sheets are presented. The specimens are subject to crack growth both in the steel and bond line. Influence of the load ratio and initial crack length on the overall endurance and debonding of the laminate was experimentally investigated. Strengthening increased the endurance of specimens up to 6.1 times and a higher load ratio was found to shorten the endurance increase. The growth rate of the debonded zone was unchanged in specimens with long initial crack lengths, thus the laminate was utilized better at any given crack length than in specimens with shorter initial cracks. Using the optical measuring equipment ARAMIS the size and shape of the debonded zone was measured at long crack lengths, proving an increasing debond growth rate close to failure.

INTRODUCTION

Fatigue in eccentrically loaded side notched plates strengthened with FRP is not yet fully understood, in fact, research on such strengthened plates is very limited. This paper investigates the influence of the load ratio $R = P_{max} / P_{min}$ and the pre-cracked length a_0 on the fatigue life of ESE(T) specimens (the eccentrically-loaded single edge crack tension specimen) strengthened with carbon fibre reinforced polymers (CFRP). Furthermore, topics as thickness of the adhesive layer and the importance of mode II crack propagation on fatigue life are discussed.

Studies of bonded repairs using FRP composites for fatigue damaged structures can be traced back to the early 70's where the method was introduced to the military and aircraft industry [1]. Mainly single sided bonded repairs were used for aircraft structures and research was concentrated on that type of repairs. Researchers succeeded in increasing the service life of aircraft components with the benefit of avoiding expensive traditional repairs and exchange of structural parts, see [2-6]. Composite materials were not only useful for aircraft structures. Strengthening of reinforced concrete structures for higher load carrying capacity initiated in the late 80's, with the purpose of rehabilitation and upgrading existing structures, [7]. Metallic structures may also need rehabilitation or upgrading, but not only for static strength. Interest grew to find a suitable solution to fatigue problems in steel structures. Bonded FRP's were adopted from the aircraft industry, and recent studies have verified the use of CFRP as a fatigue crack retardation method for steel structures, [8-13].

There are currently no design methods available for strengthened steel structures in fatigue, which can be compared to the fatigue detail categories in Eurocode 3. A strengthened detail is difficult to analyze since fatigue cracks can appear in several materials and interfaces. When considering the adhesive, some empirical rules describing the performance do exist, [14], but the overall design has not yet been fully covered. Linear elastic fracture mechanics (LEFM) for evaluation of the stress intensity factor (SIF) used in crack growth analysis is a useful tool for understanding fatigue problems arising in a strengthened structure. The accuracy of the SIF depends on the ability to predict the debonded zone. The debonded zone is the envelope of the mode II fatigue crack between the adherents. Results from finite element analysis on center cracked specimens showed that the debonded shape could be estimated as an ellipse, [15]. This was experimentally verified in [4,8]. However, this shape is not describing conditions in side-notched specimens. Side-notched specimens were tested in [5,6]. Trumpet or cone shaped debond zones were obtained for different kinds of adhesive systems, rather similar to the debonded zones found in this study. In [5], performance of the bond was found to be governing for the size of the debond zone and crack retardation effect. This emphasizes the importance of the bond since it governs the SIF and thereby the crack growth propagation in the strengthened plate.

In general, strengthening of metallic structures in fatigue with FRP materials has proven its feasibility through many years of use in the aircraft industry, but the method still needs to gain acceptance in the construction industry.

BACKGROUND

The basic theories used to design the specimen and to interpret the test results are here briefly presented. This includes LEFM, crack tip plasticity and debonding.

The essential parameter in LEFM when evaluating crack behavior is the SIF. Irwin introduced the SIF, K, to describe the singular stress field in the vicinity of a crack tip, [16]. Main governing parameters are the crack length a, geometry and loading. The SIF is dependent on the strain energy release rate, G, and can in many cases be directly interchanged following their relationship. The definition of the SIF and the simple relation to G is shown below.

$$K = \sigma\sqrt{\pi a}\, f(\tfrac{a}{w},...) \quad \text{and} \quad K^2 = EG \tag{1}$$

Here σ is the far field stress, $f(\frac{a}{w},...)$ is the geometrical correction and E Young's modulus.

On a strengthened specimen the effect of a laminate on the steel can be divided into two separate parts.

- Reduction of the stress range $\Delta\sigma$ in the steel
- Hindering of crack opening and change of crack opening shape due to the laminate stiffness

These effects reduce the SIF range ΔK.

The SIF range is a governing parameter in crack growth, which is commonly described by Paris' Law [17]. The crack growth rate is given as a straight line in a double logarithmic coordinate system, when plotting and fitting da/dN as a function of ΔK, where da/dN is the crack extension per cycle. The law is given as

$$\frac{da}{dN} = C\Delta K^m \tag{2}$$

Where *C* and *m* are experimentally determined material dependant factors.

Effect of crack tip plasticity

Fatigue crack growth may be influenced by plasticity effects near the crack tip. The plastic zone r_p contains an irreversible deformation field which results in elastic compressive stresses near the crack tip. The magnitude of the compressive stresses will yield an effective SIF given by $\Delta K_{eff} = U\Delta K$, where U is a reduction factor. This phenomenon is described in, [18]. Plasticity effects can be omitted if the size of the plastic zone is small. According to [19] LEFM is applicable for an ESE(T) specimen if $W - a \geq 4r_p$ is fulfilled. To transfer the criteria to the strengthened specimen, the plastic energy loss per load cycle is considered. When the energy loss in the strengthened specimen equals the energy loss in the reference specimen at $W - a = 4r_p$, the criteria for LEFM is reached. This is shown with a vertical line in Figure 7.

Debonding during fatigue crack growth

When a mode I fatigue crack propagates in a steel plate strengthened with FRP laminates, a mode II fatigue crack is created in the steel/FRP interface that requires the lowest amount of energy to fracture. Ratwani, determined the shape of the debonded zone to be elliptic using a critical strain, ε_C, as failure criteria in a numerical model, [15]. However, the critical fracture energy, G_C, would be a more general choice. The shape of the debonded zone was investigated on a typical test specimen from [13] with a 2mm thick epoxy adhesive layer, see Figure 1a). At Figure 1b), an area of the adhesive layer is magnified. The approximate debonded shape was visually estimated to be of elliptical shape. The observation is in correspondence with results from [4,15]. See also Figure 1c) for principle sketch of an elliptical debonded zone.

EXPERIMENTAL WORK

Fabrication of Test Specimen

The ESE(T) specimens were fabricated in accordance with [19], see Figure 2. The steel specimens were pre-cracked by cyclic loading in order to assure a sharpened fatigue crack. The length of the pre-crack is varied as shown in the test matrix in Table 3. After pre-cracking, the ESE(T) specimens were strengthened using a CFRP sheet system. The surface of the specimens was blast cleaned until SA2½ and the strengthening carried out immediately after. The CFRP composite was laid-up directly onto the ESE(T) specimen.

Thereby the same type of adhesive is used in the laminate as for the bond between CFRP and steel. This procedure results in a very thin adhesive layer between the CFRP and steel (~0.1mm). The laminate consists of six layers unidirectional carbon fiber sheets with a density of 300g/m², resulting in a thickness of 2.3mm and a stiffness increase of the specimens of 9.1%. The geometry is shown on Figure 2.

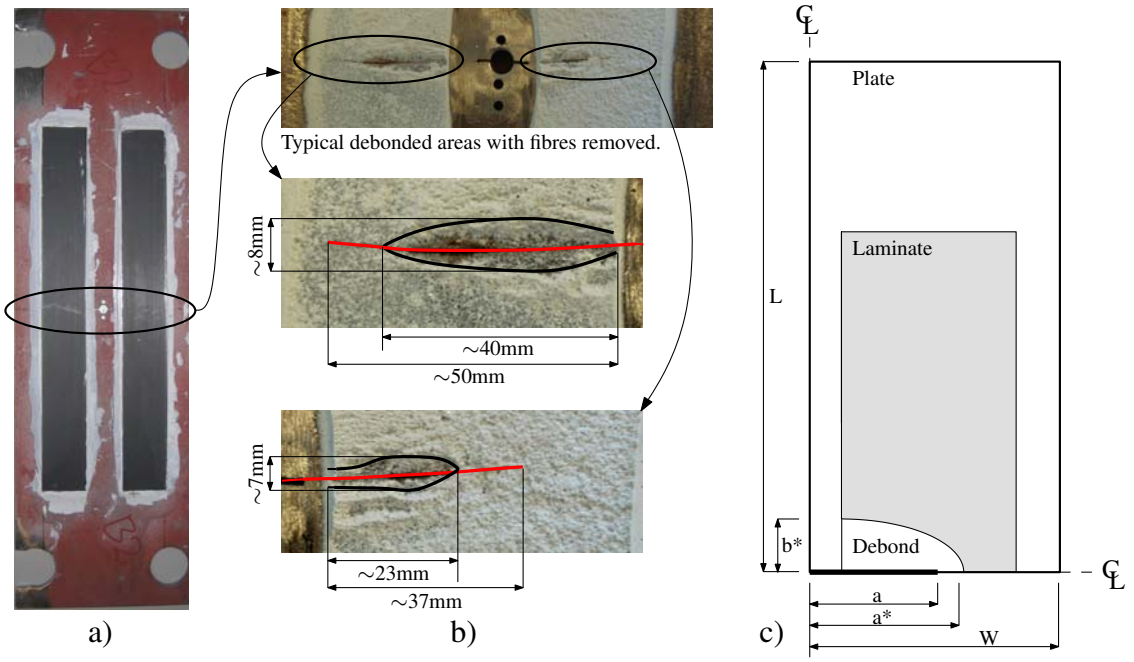

Figure 1. Visible debonded zones after removal of laminate in [13]. Red line in magnified views b), is the extension of the crack. Adhesive thickness: 2mm.

Material testing

CFRP and steel

E-modulus and strength of the laminate was determined by 14 flat tension specimens manufactured and tested in accordance with [20]. The results are shown in Table 1, where E_c is the E-modulus, E_s is the E-modulus, f_c is the tensile strength, f_{fl} is the flexural strength, E_a is the E-modulus, f_t is the tensile strength, ε_t is the failure strain, f_y is the yield strength, ε_u is the ultimate strain and f_u is the ultimate strength. Adhesive parameters are given by the supplier.

ESE(T) specimens

The ESE(T) specimens were fabricated from an 112 year old steel girder. The static mechanical properties were found from 3 dog-bone tension tests in [13], see Table 1. Through 6 fatigue tests using compact tension (C(T)) specimens in accordance with [19], Paris' equation was found suitable to describe the fatigue behavior of the steel. The SIF threshold value was determined to $\Delta K_{th} = 8\,\mathrm{MPa}\sqrt{\mathrm{m}}$, the parameters in Paris' equation are given in Table 2.

Table 1. Mechanical properties for CFRP, adhesive and steel. Adhesive parameters are 7day values at 23°C. f_y is given as upper/lower yield strength. Steel test is from [13].

	CFRP			Adhesive				Steel			
	E_c	ε_u	f_c	f_{fl}	E_a	f_t	ε_t	E_s	f_y	ε_u	f_u
	[GPa]	[%]	[MPa]	[MPa]	[GPa]	[MPa]	[%]	[GPa]	[MPa]	[%]	[MPa]
Mean	117	1.47	1722	91,5	3,3	69	6,4	210	302/ 294	15	382
STD	5.2	0.01	114								

Table 2. Parameters for Paris' law calculated from test results. The unit for *C* is $\mathrm{MPa}\sqrt{\mathrm{m}}$.

CT-no.	CT-01	CT-02	CT-03	CT-05	CT-07	CT-09
R	0.3	0.3	0.1	0.3	0.1	0.1
C	$3.64\cdot10^{-13}$	$3.32\cdot10^{-13}$	$6.01\cdot10^{-14}$	$1.34\cdot10^{-13}$	$1.10\cdot10^{-13}$	$1.03\cdot10^{-14}$
m	4.01	3.93	4.38	4.20	4.17	4.88

Test Setup

Through a pin connection the specimens are dynamically loaded with a constant load range of $\Delta P = 20\mathrm{kN}$ and two different load ratios *R*, as shown in Table 3. The CMOD (Crack Mouth Opening Displacement) was measured by a clip gauge mounted at the edge of the specimen. CMOD was converted to crack length by a compliance method as given in [19] and use of striation marks. In order to measure the development of the debonded zone, the optical measurement system ARAMIS was used. ARAMIS is an advanced image correlation system using images from two cameras to calculate a strain field on the specimen surface. Strain values were calculated with an accuracy of ±0.5%.

Table 3. Test matrix showing configuration name and parameters. P_0 is the mean load and the amplitude is $\Delta P = 20\mathrm{kN}$.

Configuration	No. of test	*R*-value	P_0	Pre-crack	CFRP Sheet	Increase in stiffness
			[kN]	[mm]	[no. of layers]	[%]
A	3	0.3	18.57	3	0	0
B	3	0.1	12.22	3	0	0
C	3	0.3	18.57	3	6	9.1
D	4	0.1	12.22	3	6	9.1
E	3	0.3	18.57	50	6	9.1
F	1	0.3	18.57	3	2	3.2
Total no of tests	17					

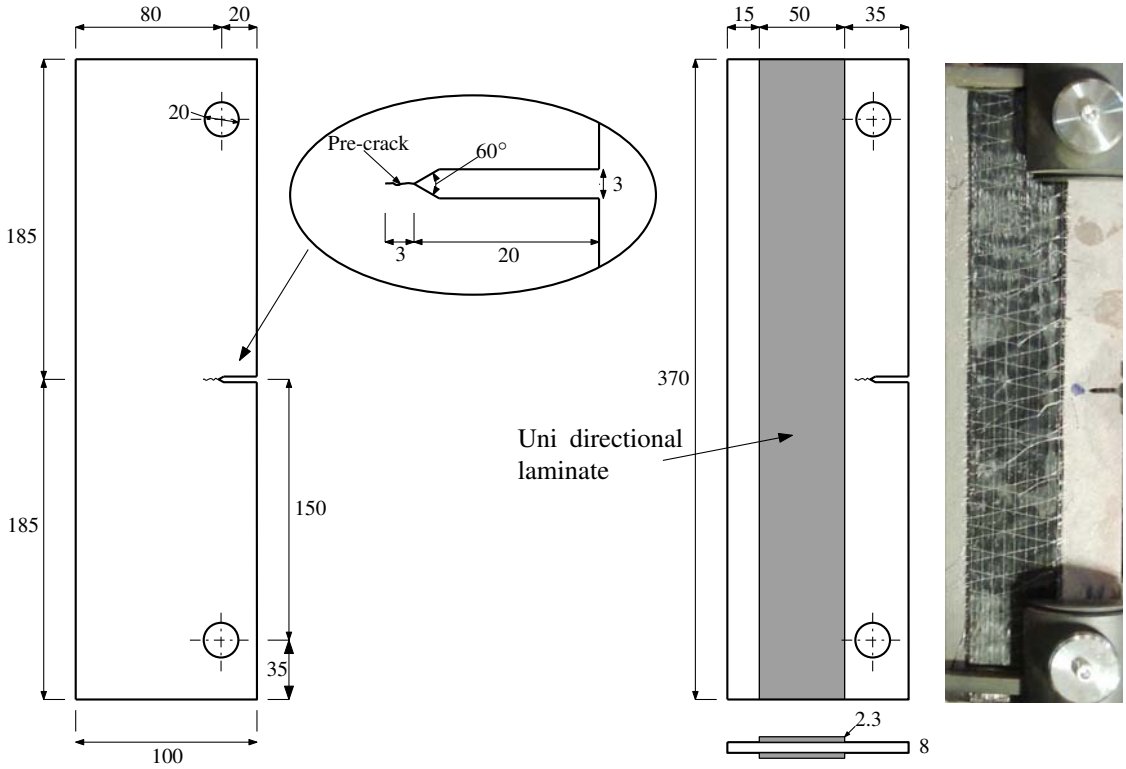

Figure 2. Geometry of reference and strengthened ESE(T) specimen, measurements in mm.

EXPERIMENTAL RESULTS

Endurance of the configurations in Table 3 is listed in Table 4 and *aN*-curves are shown in Figure 3.

Load ratio

Comparing the tests with a load ratio of R = 0.1 (configuration B and D), the endurance increase factor was 6.1. The test with the higher load ratio, R = 0.3 (configuration A and C) showed a lower endurance increase factor of 4.7. In both strengthened cases the test specimens were coinciding with similar crack growth rates. Note that specimen D1 is not considered representative for the test population of configuration D due to presence of significant residual stresses in the steel from production or machining.

Pre-cracked length

Specimens with a pre-crack of 50mm (configuration E), did not show crack growth during the first ~100,000 cycles. However, an initiation and growth of the debonded zone was observed. These cycles are plotted as a horizontal line on Figure 3. Configuration E resulted in an average endurance increase factor of 4.8 – 2% above configuration C. The crack growth rate was lower and coincident for two of the three specimens.

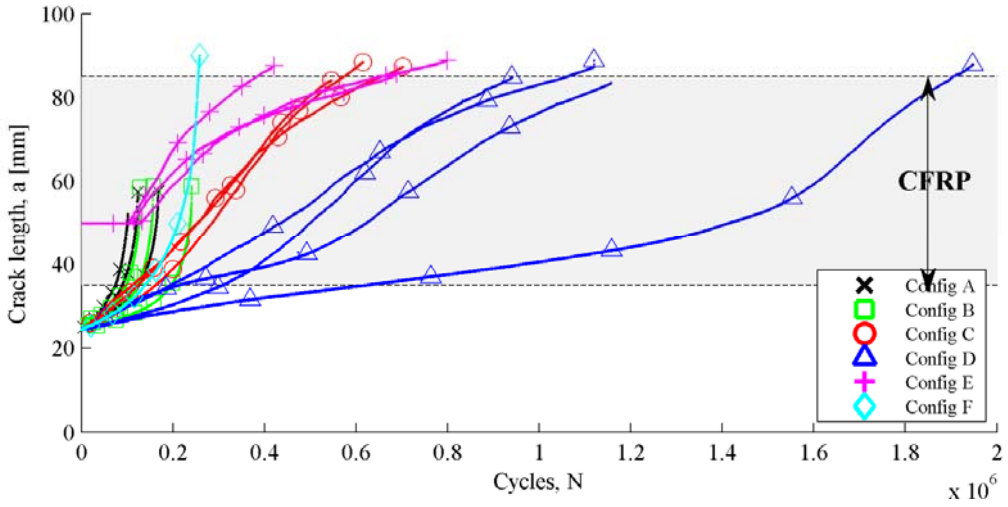

Figure 3. *aN*-curves for configuration A to F.

Table 4. Test results from all test specimens, showing the average number of cycles for each configuration and the lifetime improvement compared with the respective reference test configuration.

Config.	Unique specimen no.	*a* at failure	*N* at failure	Mean	Relative lifetime improvement	Mean lifetime factor
A1	06	57.52	167500	132800	-	1
A2	07	57.43	123400		-	
A3	18	52.21	107600		-	
B1	02	58.75	240700	175100	-	1
B2	04	58.59	128000		-	
B3	08	58.74	156600		-	
C1	03	88.40	614400	628800	362%	4.7
C2	12	87.35	702600		429%	
C3	17	84.02	569400		329%	
D1	09	87.95	1948000	1072500 (1291400)	1012%	6.1 (7.4)
D2	10	88.83	1120000		540%	
D3	16	83.57	1157000		561%	
D4	11	84.79	940600		437%	
E1	05	85.64	688600	636000	419%	4.8
E2	14	88.88	799000		502%	
E3	15	87.52	420400		217%	
F	13	90.03	258200	258200	94%	1.9

Failure modes

The reference specimens failed in a plastic failure where large deformation were present in the last couple of hundred cycles, whereas the strengthened specimens failed by debonding of the laminates. In Figure 4 the cross section at fracture is shown for a reference and a strengthened specimen. There were small traces of adhesive on the steel and on the

Figure 4. Cross section of a reference and a typical strengthened specimen after failure.

laminate, hence the debond occured in the adhesive layer. The failure initiated when the crack had propagated till about 90mm and the debonded zone in the adhesive was near the top of the specimen. The size of this debond zone at failure was apparent when studying the steel surface underneath the laminate, see Figure 5.

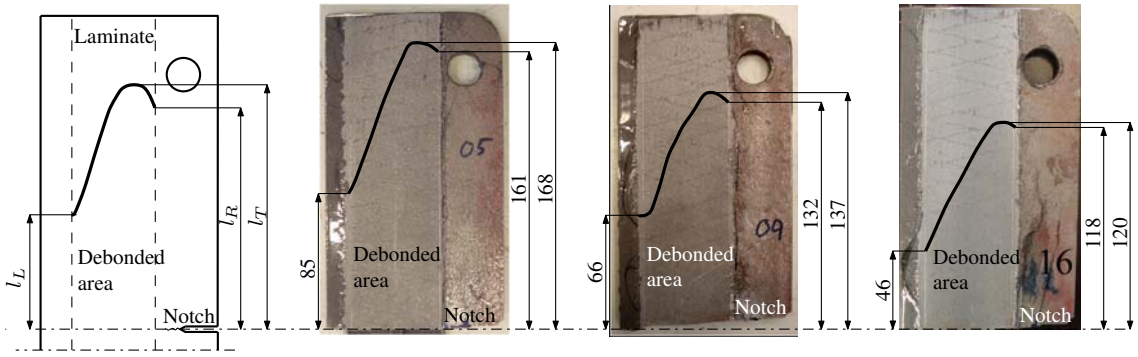

Figure 5. Typical debonding zones on specimens E1, D1, D3 at fracture.

Using the ARAMIS system, vertical strains were mapped for specimen C2 at the crack lengths 67, 71, 77 and 83mm, see Figure 6. The strain field indicates the shape and growth of the debonded zone as the crack propagates. Configuration F showed different results than the above described. An endurance increase factor of 1.9 was observed along with another failure mode; rupture in the laminate at a = 90mm.

Crack tip plasticity

Load-CMOD curves for one cycle are plotted for specimens A2 and C1 at selected crack lengths, see Figure 7. Change in CMOD value and inclination of the curves is clearly seen as the crack length increases, thus a permanent CMOD is present at the minimum load and the stiffness of the specimen is changing. At longer crack lengths, a small area between ascending and descending branches of the curves is visible.

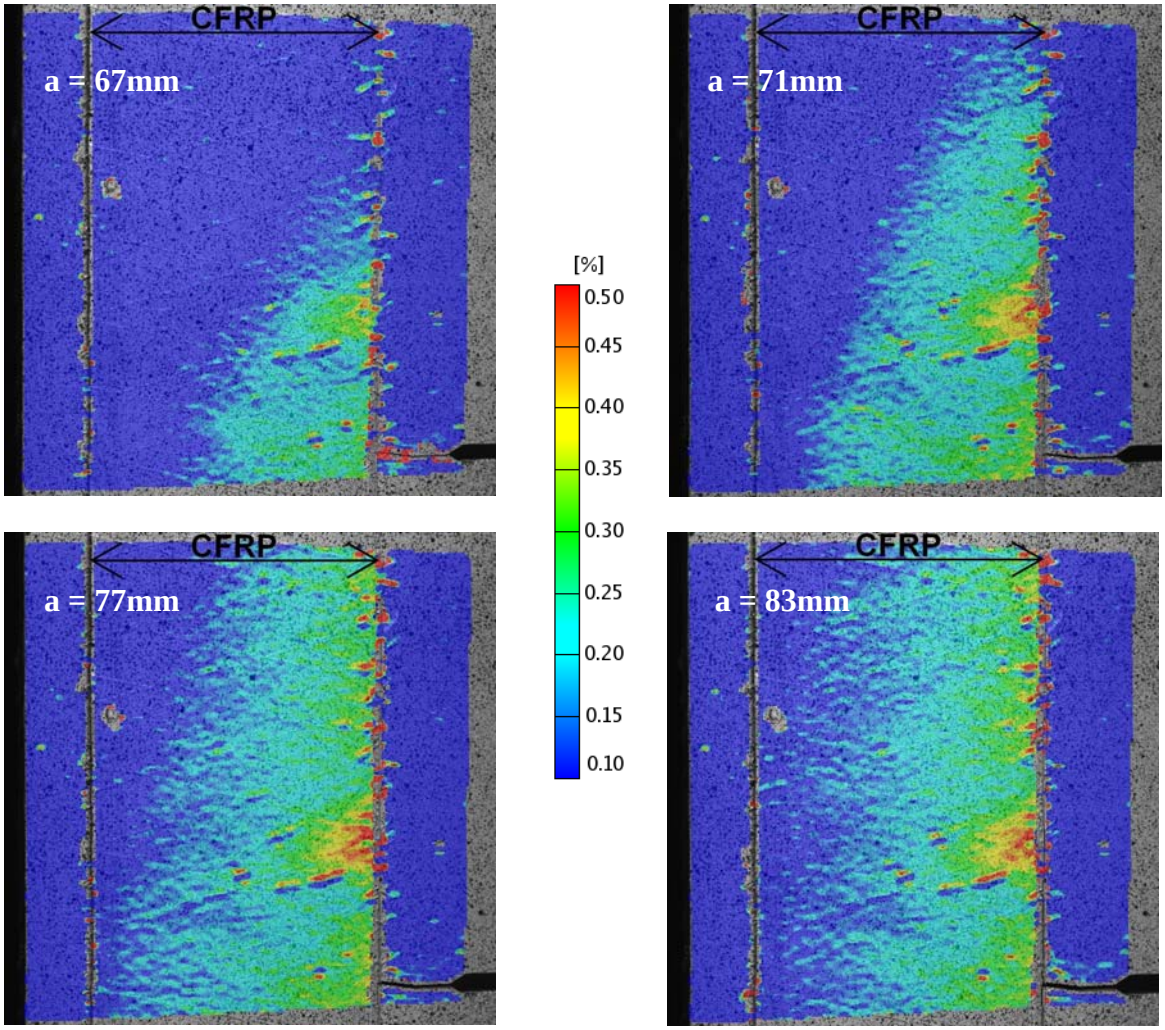

Figure 6. ARAMIS test results. Vertical strain field on the CFRP surface of the CFRP laminate indicating the debonded zone in the adhesive. The notch and crack is visible in the bottom right corner. The measured area is ~ 80x80mm.

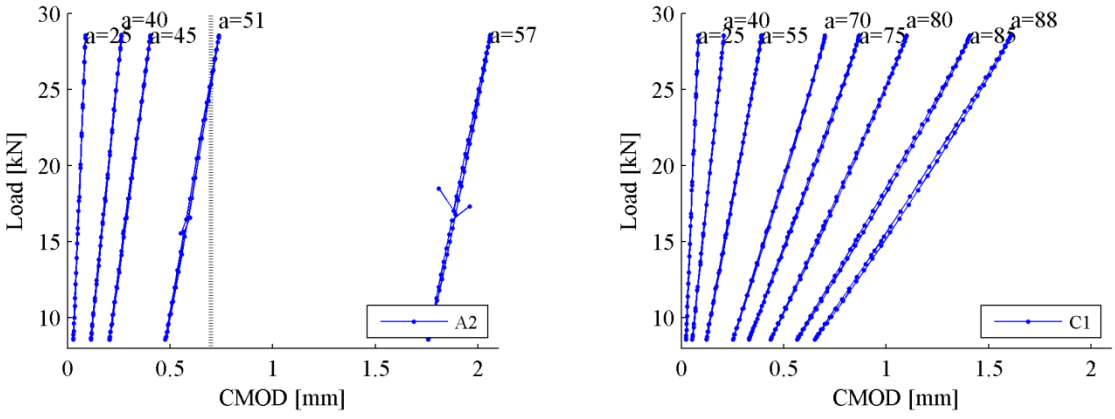

Figure 7. Load-CMOD curves of single cycles from specimen A2 and C1.

DISCUSSION

The difference in endurance between the two load ratios is a factor 1.32 for the reference specimens and a factor 1.71 for the strengthened specimens. Thereby, the effect of changing the load ratio is more distinctive for a strengthened specimen. Since a larger R-value results in higher peak stresses in the bond line, the growth of the debonded zone is likely to occur faster. In this case the SIF increases as it is depending on the debonded zone. Following Paris' equation a larger SIF yields a larger crack growth rate in the steel. Thus fatigue debonding of the laminates is depended on the load ratio.

Crack growth in specimens with a long pre-crack was divided into two phases. During the first phase crack growth in the steel was not observed, since a limited debonded zone lead to a low SIF. In phase two the debonded zone attained a size where the SIF became larger than the threshold value, resulting in combined crack growth in steel and debonded zone. This shows that the fatigue properties of the bond line are controlling parameters for the endurance of a strengthened specimen. The lower crack growth rate of configuration E compared to configuration C shows that strengthening across an existing crack is more effective, as the debonded zone is smaller in configuration E for any crack length in configuration C.

With the ARAMIS measurements the size of the debonded zone was estimated during the fatigue test. The fibers in a debonded zone have constant strain and decrease towards zero outside this. With reservations for tolerance of the measurements, the debonded zone can be estimated from Figure 6, but since the measurements are on the surface, the debonded zone is expected to be slightly larger due to shear lag. The fact that the four ARAMIS pictures were taken during the last 30mm of the crack length, is proof of a fast debond development near the end of the test. If a thicker adhesive layer had been used, shear stress in the bond line will decrease and the debonded zone will most likely grow slower. Furthermore it was a problem obtaining an accurate strain pattern due to the precision of ARAMIS. Using a higher camera resolution could solve this problem, but also open up for increasing complexities.

The limit for use of LEFM was found for the strengthened specimen. By comparing load-CMOD curves for reference and strengthend specimens at different crack lengths, the area engulfed by the increase and decrease in load during one cycle, roughly represents the energy needed to expand and compress the plastic volume. When evaluating the energy at the limit $W - a \geq 4r_p$ of the reference, the critical crack length was determined to 51mm, see Figure 7. Comparing with the energy dissapated in one load cycle in the strengthened specimen, the critical crack length was found to be 75mm. LEFM investigations are thereby at least valid until this crack length.

The test matrix was limited to two different load ratios, two different pre-crack lengths and one specimen with less strengthening. Further the same type and amount of adhesive was used for all specimens. To confirm the statements given in this paper, several more similar tests and a test matrix with a wider range of configurations is needed.

CONCLUSIONS

The results from the strengthened ESE(T) specimens proved that strengthening edge cracks with FRP laminates is possible. It was found that the increase in endurance is dependent on the load ratio and the adhesive bond, hence the propagation of the debonded zone. The effect of the load ratio was present for both reference and strengthened specimens but more significant for the strengthened specimen. This proved that a higher load ratio and thereby higher peak stresses in the adhesive bond is critical for the adherence and thereby the propagation of the debonded zone.

Configuration E with a long pre-crack experienced no crack growth in the steel at the beginning of the test, since the debonded zone had to attain a certain size before crack growth was possible. This demonstrated that it is possible to strengthen long cracks and stop the crack growth. For any given crack length, the debonded zone was smaller compared to the other strengthened configurations, thus leading to a better utilization of the laminate.

The debonded zone was seen to develop fast at large crack lengths. This result is important since the shape and size of the debonded zone is a governing parameter for evaluation of steel crack growth. Measurements by ARAMIS proved to be a successful technique to approximate the debonded zone.

Evaluation of the plastic zone led to the conclusion that elastic crack growth is distinctively extended in the strengthened specimens.

FUTURE WORK

Based on current knowledge it is concluded that the following future research will be beneficial for the understanding use of FRP materials for strengthening of structures and implementation in practical cases.

- Similar tests varying more parameters, e.g. increasing the thickness of the adhesive and changing the geometry and load conditions.
- Further investigations of the debonded zone, e.g. by further use of ARAMIS.
- Non-linear fracture mechanic modeling of mode II crack development to predict development of debond zone using cohesive elements.
- Strengthening of bolted and welded connections
- Application on full scale structures and monitoring

It is suggested that typical critical structural details are strengthened using a standardized method and SN curves as known from Eurocode 3 is extracted for practical design purposes.

REFERENCES

1. Baker, A. A., A summary of work on applications of advanced fibre composites at the Aeronautical Research Laboratories, Australia. Composites, **9(1)**, 11-16 (1978).

2. Blichfeldt, B. and McCarthy, J. E., Analytical and experimental investigation of aircraft metal structures reinforced with filament composites. Phase II – Structural fatigue, thermal cycling, creep and residual strength. Technical Report, Nasa CR-2039, 1972.
3. Ratwani, M. M., ANALYSIS OF CRACKED, ADHESIVELY BONDED STRUCTURES., Collect Tech Pap AIAA *ASME Struct Struct Dyn Mater Conf 19th*, 155-163, 1978
4. Roderick, G.L., Crack Propagation in Aluminum Sheets Reinforced with Boron-Epoxy, NASA Technical memorandum, TM-80056, 1979.
5. Baker, A. A., Repair efficiency in fatigue-cracked aluminium components reinforced with boron/epoxy patches., Fatigue & Fracture of Engineering Materials & Structures, **16(7)**, 753-765 (1993).
6. Baker, A.A., Bonded Composite Repair of Metallic Aircraft Components – Overview of Australian Activities., AGARD-CP-550, Paper 1, 1–14, 1995,
7. Kaiser, H., Bewehren von Stahlbeton mit Kohlenstoffasverstärkten Epoxidharzen (in German), Phd Dissertation, ETH Nr. 8918, ETH Zürich, 1989.
8. Bassetti A., Lamelles precontraintes en fibres carbone pour le renforcement de ponts rivetes endommages par fatique. [in French], PhD Thesis, Ecole Polytechnique Federale de Lausanne, Lausanne, 2001
9. Tavakkolizadeh M, Saadatmanesh H., Fatigue strength of steel girders strengthened with carbon fiber reinforced polymer patch., Journal of Structural Engineering., **129(2)**, 2003.
10. Domazet, Z, Comparison of Fatigue Crack Retardation Methods, Engineering Failure Analysis, **3(2)**, 137-147, 1996
11. Jones S. C., Civjan S. A., Application of fiber reinforced polymer overlays to extend steel fatigue life., J Compos Construct, **7(4)**, 2003
12. Liu, H.B., Xiao, Z.G., Zhao, X.L., Al-Mahaidi, R., Fracture Mechanics Analysis of Cracked Steel Plates Repaired with Composite Sheets, *First Asia-Pacific Conference on FRP in Structures.*, 2007
13. Täljsten, B., Hansen, C.S., Schmidt, J. W., Strengthening of old metallic structures in fatigue with prestressed and non-prestressed CFRP laminates, Construction and Building Materials., **23(4)**, 1665-1677, 2009.
14. Deng, J. & Lee, M. M., Fatigue performance of metallic beam strengthened with a bonded CFRP plate., Composite Structures, **78(2)**, 222-231, 2007
15. Ratwani, M. M., Characterization of Fatigue Crack Growth in Bonded Structures, Volume II: Analysis of Cracked Bonded Structures, AFFDL-TR-77-31, Air Force Flight Dynamics Laboratory, Ohio, 1977.
16. Irwin, G. R., Analysis of Stresses and Strains Near the End of a Crack Traversing a Plate. Journal of Applied Mechanics, **24**, 361-364 (1959).
17. Paris, P., Erdogan, F., A Critical Analysis of Crack Propagation Laws., Journal of Basic Engineering, **85**, 528-534 (1963).
18. Elber, W., The Significance of Fatigue Crack Closure, ASTM 486, 230-242, 1971.
19. ASTM Committe E08, 1978, E647 – 0: Standard Test Method for Measurement of Fatigue Crack Growth Rate, ASTM International, 2000.
20. ACI 440.3R-04, Guide Test Methods for Fiber-Reinforced Polymers (FRPs) for Reinforcing or Strengthening Structures, American Concrete Institute, 2004